Characterisation of the interactions of aromatic amino acids with diacetyl phosphatidylcholine†

John M. Sanderson* and Eleanor J. Whelan

Department of Chemistry, University Science Laboratories, South Road, Durham, UK.
E-mail: j.m.sanderson@durham.ac.uk; Fax: +44 191 3844737; Tel: +44 191 3342107

A simple bimolecular system for characterising the interactions of amino acids with diacyl-3-phosphatidylcholines has been developed. The system contains two components: an *N*-acetyl amino acid *N*′-alkyl amide and diacetyl-3-*sn*-phosphatidylcholine (DAPC). Interactions between a series of aromatic amino acids and DAPC have been characterised by ^{1}H NMR techniques. Of the amino acids examined, tryptophan and tyrosine were shown to have particularly favourable interactions with the DAPC choline headgroup. Our observations are consistent with the previously reported tendency for these amino acids to occur preferentially at the lipid-water interface. Using data from ROESY experiments and complexation-induced chemical shift changes, we have been able to generate molecular models for the tryptophan–DAPC adduct that are consistent with the observed results. The adduct is characterised by amide carbonyl–cation interactions, hydrogen bonding and cation–π interactions.

Introduction

Several recent reports have suggested that aromatic amino acids play an important role in directing interactions between proteins and lipids in the region of the polar headgroups, at the interface of the low-dielectric interior of the lipid bilayer and the high-dielectric bulk aqueous phase.[1a–d] A diverse array of membrane properties may be influenced by these amino acids through their interactions with lipids, including the formation of lipid domains,[2] lipid redistribution through hydrophobic mismatch,[3a,b] the stability of β-barrel membrane proteins,[4] the activity of antimicrobial peptides, particularly with respect to haemolytic activity,[5a,b] and the binding of bacteriophage to the membranes of prokaryotes during infection.[6] Although there have been many reports in the literature concerning the nature of peptide-lipid interactions, most work has centred around physical measurements on systems composed of small peptides or whole proteins and lipid membranes.[7a–e] There has been little work directed towards the development of a simple system that can be used to determine the strength and preferred geometry of the weak non-covalent interactions of individual amino acids with lipid headgroups in non-competing solvents. In this paper we describe such a system.

We were initially intrigued by observations that certain aromatic amino acids, especially tryptophan and tyrosine, have a non-uniform distribution in membrane proteins,[8a,b] with a higher than average tendency to occur in the interface region around the lipid headgroups. We therefore designed a model system that would enable us to probe the interactions of these amino acids with neutral lipids. Our system comprised low molecular weight peptide and lipid analogues that were soluble in non-competitive NMR solvents (such as CDCl₃) and preserved all of the chemical functionality present in the natural systems (Fig. 1). This system would enable us to determine whether aromatic amino acids have specific interactions with phosphatidylcholines that are more favourable in free energy terms than other amino acids, through the use of host–guest

titrations with amino acid–lipid pairings. We selected analogues of tyrosine, tryptophan and phenylalanine as examples of aromatic amino acids, and valine as a non-aromatic control. The shortest chain lipid, diacetyl-3-*sn*-phosphatidylcholine (DAPC), was chosen as the lipid analogue of choice, principally because of its good chloroform solubility free from complications arising from micellisation, but also because its water solubility would will enable us to perform experiments in water if required. All of these analogues were synthetically amenable and readily prepared in suitable quantities for NMR studies.

Experimental

Synthesis of compounds

All compounds used have been previously described in the literature:

1,2-Diacetyl-*sn*-glycero-3-phosphocholine[9] (DAPC, **1**): CA 54672-38-7; *N*-acetyl-L-tyrosine ethylamide[10] (**2**): CA 49577-69-7; *N*-acetyl-L-tryptophan ethylamide[11] (**3**): CA 96384-15-5; *N*-acetyl-L-phenylalanine ethylamide[12] (**4**): CA 29744-08-9; *N*-acetyl-L-valine ethylamide[13] (**5**): CA 38075-78-4.

The water content of DAPC was determined by thermogravimetric analysis using a Perkin-Elmer Pyris 1 analyzer.

Determination of adduct stoichiometry

In order to determine the stoichiometry of the adducts formed between DAPC (**1**) and each of the amino acids **2–5**, a series of solutions of constant total molar concentration were prepared
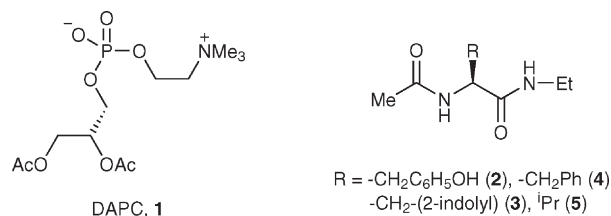

Fig. 1 Host–guest systems used in this study.

† Presented at the Biophysical Chemistry Conference 2003, Warwick, UK, July 21–23, 2003.

that contained varying ratios of **1** and **2**–**5**. Job plots were then made of the observed chemical shift change ($\chi \Delta \delta_{obs}$) against mole fraction (χ).[14] The maxima of these plots were used to determine adduct stoichiometry.

NMR titrations

Host–Guest titrations[14,15] were performed in duplicate in $CDCl_3$ on a 200 MHz Varian Mercury 200 spectrometer. A 2 ml sample of the host was prepared at a known concentration (typically 2–12 mM), and 1 ml of this was used to prepare a solution of the guest at a known concentration (typically 100–150 mM). Aliquots of the guest solution (containing host) were then added successively to 0.5 ml of the host solution and the ^1H NMR spectrum recorded after each addition. DAPC was generally used as the guest due to its good solubility in $CDCl_3$, although reverse titrations using **3** and **4** as guest were also performed to estimate the complexation-induced chemical shift changes. Amino acid derivatives **2** and **5** had low association constants with DAPC or were insufficiently soluble in $CDCl_3$ for meaningful results to be obtained when these were used as guest. Signals that exhibited a chemical shift change of more than 0.04 ppm during the course of the titration were subjected to non-linear curve fitting procedures using the Solver function in the program Excel (Microsoft Corp.). The observed chemical shift data (δ_{obs}) for 1:1 complex formation were fitted to eqn. (1), where K is the association constant, [G] is the guest concentration, δ_{free} is the free chemical shift of the host, and δ_{obs} is the limiting bound chemical shift in the 1:1 complex. The observed chemical shift data (δ_{obs}) for 2:1 complex formation were fitted to eqn. (2), where K_1 and K_2 are the microscopic association constants, [G] is the guest concentration, [HG] is the concentration of the 1:1 complex, δ_{free} is the free chemical shift of the host, and δ_{obs1} and δ_{obs2} are the limiting bound chemical shifts in the 1:1 and 2:1 complexes respectively. The data for 1:2 complex formation (*i.e.* with DAPC as host) were fitted to eqn. (3).

The association constant for each experiment was evaluated as the weighted mean based on the observed change in chemical shift for all signals monitored. The error was taken as twice the standard error. For signals that exhibited a chemical shift change of less than 0.04 ppm, the calculated association constant was used for non-linear curve fitting procedures for the sole purpose of determining the maximal complexation-induced change in chemical shift.

$$\delta_{obs} = \left[\frac{K[G](\delta_{obs} - \delta_{free})}{1 + K[G]} \right] + \delta_{free} \qquad (1)$$

$$\delta_{obs} = \left[\frac{K_1[G](\delta_{obs1} - \delta_{free}) + 2K_2[HG](\delta_{obs2} - \delta_{free})}{1 + K_1[G] + 2K_2[HG]} \right] + \delta_{free} \qquad (2)$$

$$\delta_{obs} = \left[\frac{K_1[G](\delta_{obs1} - \delta_{free}) + K_1K_2[G]^2(\delta_{obs2} - \delta_{free})}{1 + K_1[G] + K_1K_2[G]^2} \right] + \delta_{free} \qquad (3)$$

2D ROESY spectroscopy‡

A saturated solution of the host–guest mixture in $CDCl_3$ was prepared, degassed and stored under nitrogen. ROESY experiments were recorded on a Varian Inova 500 with a 500 s mixing time, 3 s relaxation delay between pulses and 148 ms acquisition time.

‡ The authors would like to thank A. Kenwright and I. H. McKeag for help with NMR experiments.

Molecular modelling

Mechanics calculations were performed using the Tinker software package[16] and the CHARMM27 force field implementation.[17] This force field is optimised for both lipids and amino acids. To reduce the computation time, amino acids were modelled as *N*-methyl amides rather than *N*-ethyl amides. The distance limits for protons exhibiting intermolecular cross peaks in the 2D ROESY spectrum were restrained as follows according to the magnitude of the cross peak: strong ≤ 4.2 Å; medium ≤ 4.7 Å; weak ≤ 5.3 Å. Relatively large upper distance limits were chosen, as bias in the intensity of the rOe crosspeaks could not be ruled out due to the long mixing time needed to observe rOe contacts between weakly-interacting small molecules. The magnitude of the cross-peak was assigned subjectively according to visual inspection of the 2D pectrum. In order to simplify the calculations and avoid complications from the application of distance restraints to diastereotopic protons, the distance restraint was applied to the carbon atom bonded to the diastereotopic proton rather than the proton itself and relaxed by 1.12 Å (the aliphatic C–H bond length). The NH–Cα coupling constant was also extrapolated from the titration data to generate restrictions for the ϕ bond angle of the amino acid. An initial structure was generated using the Tinker 'Optimise' routine, and then subjected to repeated simulated annealing protocols. Atomic weight factors were set to the minimum value that would allow the calculation to proceed to completion without producing energy values too high to be computed. The following parameters were used to generate an initial set of 30 structures: initial temperature 1000 K, final temperature 0 K, sigmoidal cooling curve, atomic masses increased by a factor of $10^{0.05}$. These structures were sorted into groups of less than 4.0 Å RMS deviation. The lowest energy structure in each group was subjected to further simulated annealing routines (initial temperature 300 K, final temperature 0 K, exponential cooling curve, atomic masses increased by a factor of $10^{1.3}$) to generate a further set of 11 structures. The lowest energy structure in each of these sets was subjected to semi-empirical geometry optimisation without restraints using the CAChe MOPAC application (Fujitsu Limited, 2000–2002) with a PM3[18] Hamiltonian. Analytical gradients were used, and the EF method applied for optimisation. Mechanics corrections were applied to –HNCO– groups.

Results and discussion

Adduct stoichiometry

The **2**:DAPC mixture produced Job plots with maxima at mole fractions of 0.60 and 0.61 for the –NHAc and –NHEt protons respectively (Fig. 2a). Although chemical shift changes were observed for the choline protons, these were not large enough to allow meaningful analysis by Job's method. Nevertheless
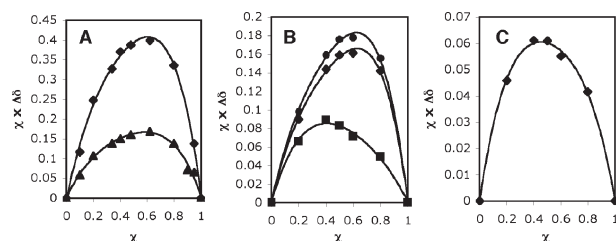
Fig. 2 Job plots for mixtures of amino acid derivatives **2**–**5** with DAPC in $CDCl_3$. The plots show the observed chemical shift change ($\Delta\delta$) of a proton as a function of mole fraction (χ) of the species bearing the proton. (a) **2**:DAPC. (b) **3**:DAPC. (c) **4**:DAPC. Data shown are for the following protons: ◆ = –NHEt, ▲ = –NHAc, ■ = –NMe₃, ● = indole-NH. Valine (**5**, not shown) produced data similar to **4**.

these protons tended towards maxima at a mole fraction of ~0.45. Together, these data either reflect the formation of a 2:1 adduct that possibly exhibits some non-ideal behaviour, or the formation of multimeric structures (2:2, 2:3 *etc.*). The titration data produced a considerably better fit for the 2:1 adduct than for other stoichiometries however (Fig. 3a and 3b), and the adduct stoichiometry was therefore considered to be 2:1. Non-ideality may have been expected in the behaviour of the **2**:DAPC complex as **2** was used close to its solubility limit (3 mM in $CDCl_3$).

The **3**:DAPC Job plot (Fig. 2b) produced maxima at 0.65, 0.65 and 0.35 for the for the indole-NH, –NHEt and –NMe_3 protons respectively, which was consistent with the formation of a 2:1 adduct. The **4**:DAPC mixture produced data consistent with a 1:1 stoichiometry (Fig. 2c), as did the **5**:DAPC mixture (data not shown).

NMR experiments

For all titrations, good fits of the calculated isotherms to the experimental data could be produced, allowing association constants and complexation-induced chemical shift changes to be determined. We were concerned that the water content of the DAPC sample may influence the observed association constants, particularly considering the hygroscopic nature of DAPC, and therefore performed thermogravimetric analysis of each DAPC sample used. Reproducible association constants were obtained in the titrations described above using a DAPC sample that contained 12% H_2O by weight. Examples of the titration isotherms are presented in Fig. 3.

The titration data are summarised in Table 1.

Phenylalanine and valine

Both the phenylalanine derivative (**4**) and the valine derivative (**5**) produced adducts with significantly weaker association constants and smaller complexation-induced chemical shift changes than either **2** or **3**. The downfield shifts of the amide protons were the only complexation-induced changes of note.
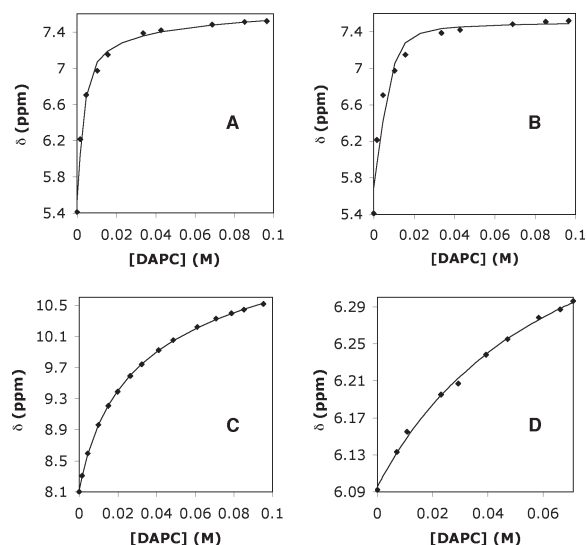
Fig. 3 Examples of binding isotherms with DAPC as the guest, showing the observed chemical shift (δ) as a function of DAPC concentration. In all cases, the observed data are plotted as points, and the calculated data from non-linear least squares fitting aa a line without points. (a) data for the –NHEt amide proton in the titration of **2** ([**2**] = 5.3 mM) fitted to a 2:1 binding isotherm. (b) as *(a)*, but fitted to a 1:1 binding isotherm. (c) data for the indole-NH of **3** ([**3**] = 12.2 mM). (d) data for the –NHEt amide proton in the titration of **5** ([**5**] = 8.5 mM).

Compound **4** was sufficiently soluble to be used as a guest in a reverse titration. In this case, none of the chemical shift changes observed for DAPC were greater than ±0.06 ppm. These data are consistent with relatively non-specific hydrogen bonding or carbonyl-cation interactions between these amino acids and the lipid.

Tyrosine

Tyrosine analogue **2** formed a 2:1 adduct with relatively high values for both microscopic association constants K_1 and K_2, particularly when compared with the valine K_1 association constant. Some pronounced downfield complexation-induced chemical shift changes were observed, particularly for the amide protons, the chemical shift changes of which were greater than those of either the phenylalanine or the valine adducts with DAPC. Smaller shift changes were observed for the aromatic protons. Although a reverse titration could not be performed, the small chemical shift changes observed for the choline group in the Job plot (see above) indicate that at best the aromatic ring has a very weak interaction with the choline group. The data could be interpreted as indicative of a hydrogen bonding interaction between the phenolic proton and the phosphate oxygen, and hydrogen bonding or carbonyl-cation interactions between the amides and the quaternary ammonium centre of the choline. The phenolic proton was too broad to be observed during these titrations however, and unambiguous rOe contacts could not be observed in the ROESY spectrum, due to superposition of the signals from the DAPC ammonium methyl groups and the methylene protons of the amino acid ethyl group, which may have obscured genuine contacts. Further work will be needed to characterise this interaction.

Tryptophan

Tryptophan analogue **3** formed a 2:1 adduct with association constants that were significantly higher than those of either valine or phenylalanine. Significant complexation-induced chemical shift changes were observed for all of the amide and aromatic protons, with the indole-NH producing the largest shift change that was observed during these titrations. The association constant for the formation of the 2:1 adduct (K_2) was considerably higher than that of the 1:1 adduct (K_1), which may reflect a smaller decrease in conformational entropy of the lipid upon binding of the second tryptophan molecule to the 1:1 adduct. Implicit in this argument is formation of the 1:1 adduct through specific, directional interactions. The difference in complexation-induced chemical shift changes for the formation of 1:1 and 2:1 adducts indicates that the two tryptophan binding sites are not identical, although for most protons the shift changes are in the same direction in both cases. Two protons have shift changes in opposite directions for the 1:1 and 2:1 adducts. Interestingly, both of these are protons on the phenyl part of the indole ring (protons 4 and 7 in Table 1), which suggests that the environment of the indole ring differs most between the two adducts.

Tryptophan analogue **3** was soluble enough in $CDCl_3$ to allow it to be used as a guest in a reverse titration. Around 55% of the binding isotherm could be explored in this titration, and as a consequence association constants could not be calculated meaningfully. Nevertheless the complexation-induced chemical shift changes of the lipid could be estimated. Significant negative chemical shift changes for all of the protons of the choline headgroup were observed (between −1.0 and −0.2 ppm). The large downfield shift changes observed for the indole –NH and the amide protons, and the upfield chemical shift changes for the protons of the choline group in the reverse titration are consistent with a combination of specific hydrogen bonding and cation–π interactions between **3** and DAPC.

Table 1 ^{1}H NMR titration data for adducts between DAPC and **2–5**^{a}

| Host	Guest	K_1/M^{-1}	K_2/M^{-1}	$\Delta\delta_1$/ppm		$\Delta\delta_2$/ppm	
(Structure: N-acetyl tyrosine N-ethylamide, positions 1–9, OH)	DAPC	170 ± 29	235 ± 30	1: +2.26, 3: −0.06, 5: 0.0, 7a: −0.03, 8: 0.0,	2: +1.61 4: −0.02 6: +0.05 7b: 0.03 9: −0.02	1: +2.35, 3: −0.07, 5: +0.23, 7a: −0.30, 8: +0.15,	2: +0.59 4: +0.20 6: +0.13 7b: 0.03 9: −0.08
(Structure: N-acetyl tryptophan N-ethylamide, positions 1–13, NH)	DAPC	19 ± 2	179 ± 21	1: +2.81, 3: −0.13, 5: +0.04, 7: +0.66, 9: +3.92, 11: −0.25, 13: −0.25	2: +1.68 4: −0.21 6: +0.14 8: +0.13 10: +0.08 12: −0.26	1: +0.76, 3: −0.02, 5: +0.05, 7: −0.42, 9: +1.09, 11: −0.02, 13: −0.05	2: +0.44 4: +0.09 6: +0.07 8: +0.11 10: +0.06 12: −0.06
(Structure: phosphocholine diacetate, positions 1–8, NMe₃⁺)	**3**^{b}	—	—	1: −0.51, 3: −0.21, 5: +0.04, 6b: −0.03, 8: −0.06	2: −0.62 4: +0.06 6a: −0.03 7: −0.04	1: −0.44, 3: −0.15, 5: 0.0, 6b: −0.03, 8: −0.06	2: −1.02 4: +0.03 6a: +0.01 7: −0.04
(Structure: N-acetyl phenylalanine N-ethylamide, positions 1–8)	DAPC	18 ± 7	—	1: +0.24, 3: −0.01, 5: −0.02, 7: 0.0	2: +0.16 4: 0.01 6: 0.0 8: −0.01	—	
(Structure: phosphocholine diacetate, positions 1–8, NMe₃⁺)	**4**^{b}	—	—	1: −0.02, 3: 0.0, 5: −0.01, 6b: −0.02, 8: −0.06	2: −0.02 4: 0.0 6a: −0.01 7: −0.03	—	
(Structure: N-acetyl valine N-ethylamide, positions 1–8)	DAPC	21 ± 6	—	1: +0.50, 3: −0.02, 5: −0.03, 7: +0.03,	2: +0.37 4: 0.0 6, −0.06 8: −0.07	—	

^{a} Experiments were performed in CDCl$_3$ at 298 K. ^{b} Sufficient exploration of the binding isotherm was not possible due to low guest solubility. Binding constants determined in the reverse titration with DAPC as guest were used for curve-fitting to determine complexation-induced chemical shift changes.

2D ROESY experiments were performed on mixtures of **3** with DAPC. As with mixtures of **2** and DAPC, we experienced some problems due to peak superposition, but we were nevertheless able to produce unambiguous evidence of intermolecular rOe contacts (Fig. 4). These were not surprisingly, very weak, but considering the relative binding constants for K_1 and K_2, could be considered to have arisen from the 2:1 adduct.

Molecular modelling

The rOe contacts observed in the ROESY spectrum of **3** and DAPC (Fig. 5) were used to generate distance restraints for

mechanics calculations. The calculated NH–Cα coupling constant in the 2:1 adduct was 9.5 Hz, which reflected an average of the value for each of the molecules of **3** in the complex. Given that this was close to the predicted limiting coupling constant for a β-sheet, the ϕ angle of both of the amino acids in the adduct was restricted to between −95° and −145°. Five groups of homologous structures were obtained by simulated annealing procedures, which represent low energy conformations along multiple dynamics trajectories. These all represent plausible structures for $\mathbf{3}_2$:DAPC adducts, but nevertheless they share some common features (Fig. 6):
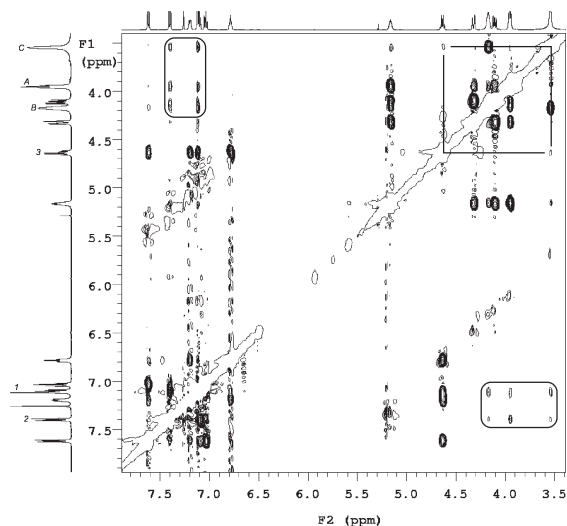
Fig. 4 2D ROESY spectrum of the **3**:DAPC mixture. Intermolecular cross-peaks are highlighted by rectangular boxes or by straight lines between them along the F1 and F2 axes.

1. The unsymmetrical nature of the adduct.

2. Cation-π interactions with at least one of the indole rings.

3. Interactions between an indole-NH and a phosphate oxygen.

4. Interactions between an amide carbonyl group and the choline ammonium group.

Additionally, some of the complexes displayed interactions between one of the alkyl amide-NH protons and a phosphate ether oxygen. It was noticed that in some of the structures produced by simulated annealing, the N–H bond of the indole was slightly out of plane with the aromatic ring. In order to examine the possibility that this was an artefact of the force field, which is not ideally suited to interactions that may involve polarisation of electron density, the lowest energy structure from each of the five groups of structures generated by annealing was subjected to semi-empirical minimisation using MOPAC/PM3 without any bond or distance restraints. In all cases, structures were produced (Fig. 7) that did not differ significantly from the CHARMM structures, and non-planar N–H bonds were maintained (see Fig. 7a and 7c, for example). Further work will be required to determine whether this is a real effect or not, but it is clear both from our results and from previous work,[19] that there is a need for force fields that are more suitably parameterised for performing calculations on lipids and aromatic systems where polarisation is likely to be an issue.

All of the amides in these models are involved in either hydrogen bonding or carbonyl–cation interactions with the
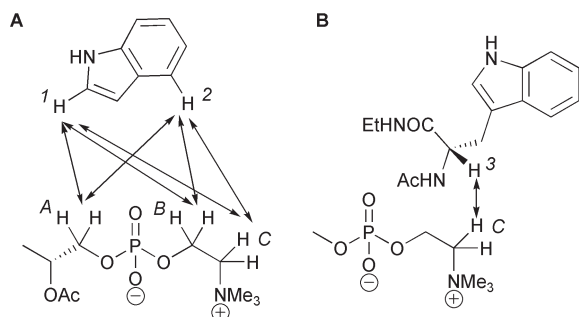
Fig. 5 Contacts observed between **3** and DAPC in the 2D ROESY spectrum. Protons giving cross-peaks are indicated by double-headed arrows. Proton labelling corresponds to the assignments in Fig. 4. (a) Contacts to the indolyl group. (b) Non-aromatic contacts.
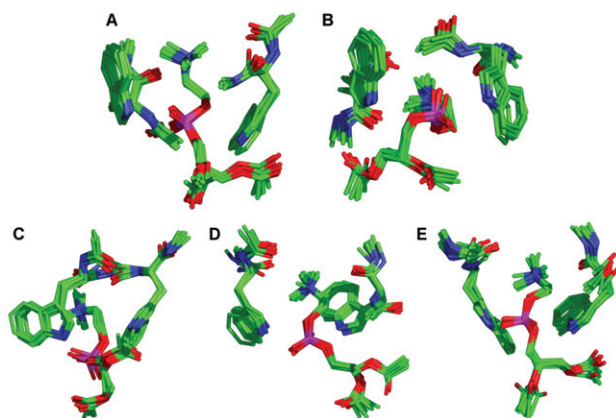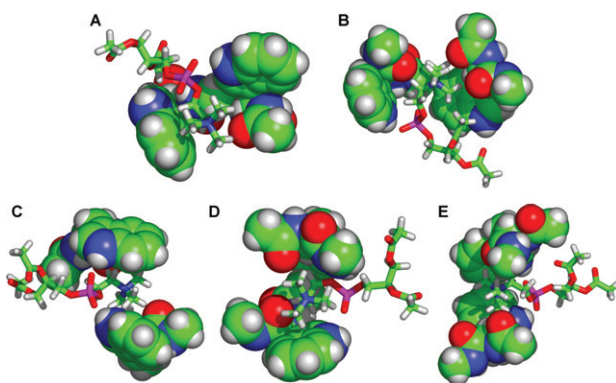

Fig. 6 Structures for the **3**$_2$:DAPC complex generated by simulated annealing. Each group of structures in A–E contains ten low-energy conformers.§

lipid, and the indole–NH protons are always hydrogen bonded to the phosphate group of the lipid. These observations are consistent with the downfield proton shifts observed during titrations. Symmetrical adducts are not formed between **3** and DAPC because of steric restrictions and the preferred staggered conformation of the –CH$_2$–CH$_2$– methylenes of the choline headgroup.

As a result, only one of the aromatic rings is usually in close contact with the choline headgroup, which accounts for the different patterns of chemical shift change observed for the indole group. Another key feature of these models is the restriction of the interactions between the amino acid and the lipid to the choline part of the lipid. As this part of the lipid molecule is achiral, this suggests that either isomer of tryptophan should interact well with DAPC, and is consistent with observations that D-analogues of antimicrobial peptides interact with membranes equally well as their L- counterparts.[20]

It is clear however, given the large chemical shift change for the indole-NH, that this is one of the critical parts of the amino acid that drives the interaction with lipids through hydrogen bonding to the phosphate. The indole ring of tryptophan is sufficiently large to form this hydrogen bonding interaction whilst maintaining close contact with the choline ammonium group. Such a cation–π interaction involving tryptophan is well precedented.[21a,b] Studies on the binding of benzene to alkali metal cations[22a,b] suggest that cation–π interactions are often more favourable in free energy terms than anticipated, and can compete favourably with water in certain

Fig. 7 Structures for the **3**$_2$:DAPC complex generated by semi-empirical minimisation of the lowest energy structures in Fig. 6. The lipid is represented by sticks and the amino acid as spacefilled spheres.§

§ These images were prepared using the program PyMol, DeLano Scientific, San Carlos, CA, USA. http://www.pymol.org/.

circumstances. It is interesting to speculate that binding of tryptophan to choline may be sufficient to displace some of the water molecules bound to the lipid.

Conclusions

The data we have obtained are entirely consistent with previous reports of the non-uniform distribution of amino acids in membrane proteins, in which the distribution of tryptophan and tyrosine is biased towards the lipid interface, with phenylalanine showing no preference for either the membrane interface or the lipid interior.[8a] In particular, we have found that both tryptophan and tyrosine exhibit significantly stronger interactions with the choline groups of neutral lipids than either phenylalanine or valine. The data for phenylalanine indicate that its interactions with DAPC are not significantly stronger than the non-aromatic valine. The interactions of tryptophan in particular, involve a combination of hydrogen bonds, cation–carbonyl interactions and cation–π interactions. These weak interactions have been observed in a non-competitive solvent in the presence of water. Further work will be required to determine whether water is displaced during the process of amino acid binding, but we are nevertheless content that binding is significant in the presence of water in a dielectric environment that lies between that of the lipid interior and bulk water. The weak binding of phenylalanine and valine to DAPC indicate that cation-carbonyl interactions are likely to contribute the least towards adduct formation. The most significant interactions that drive adduct formation for tryptophan and tyrosine involve hydrogen bonding between the phosphate group and polarised hydrogen atoms bonded to heteroatoms proximal to the aromatic system. Tryptophan is unique in forming adducts that are stabilised by cation-π interactions. The contribution of these to adduct formation is likely to be significant based on the documented interaction energies (≤ 4 kcal.mol^{-1}) of tryptophan with similar cationic species.[23] Our data reflect the *preferred* interactions of tyrosine and tryptophan with neutral phosphatidylcholines in ideal conditions, and as such are a useful starting point for the development of peptide analogues with tailored properties.

Although amino acids in regular protein secondary structure elements (helix or sheet) would not have backbone amides available for hydrogen bonding or cation-carbonyl coordination, this would not necessarily be the case in regions of extended structure or turns. Consequently, these areas may be of greater importance for lipid interactions than regular secondary structure elements. Considering that the choline group of the lipid is the only segment to interact with tryptophan, it is reasonable to expect that interactions of phosphocholine (a commonly used additive in buffers used for crystallisation) with tryptophan should be observable in crystal structures in the PDB. An initial screen of the PDB provided good examples of such interactions, alongside interactions with tyrosine, in two proteins: leukocidin F (3LKF,[24] involving Trp176 and Tyr179 of chain A) and an immunoglobulin Fab–PC complex (2MCP,[25] involving Tyr33 and Trp107 of chain H and Tyr100 of chain L). In both cases, the structures support the observations described in this paper. The phenolate oxygens of the tyrosine residues in these structures are oriented towards the phosphate oxygen atoms, and the indole rings of the tryptophan residues lie in close contact with the phosphocholine ammonium group. In 3LKF, the indole nitrogen is in very close proximity to the phosphate group, almost certainly indicating the presence of a hydrogen bond.

References

1 (*a*) W. Jing, H. N. Hunter, J. Hagel and H. J. Vogel, *J. Peptide Res.*, 2003, **61**, 219; (*b*) M. R. R. de Planque, J.-W. P. Boots, D. T. S. Rijkers, R. M. J. Liskamp, D. V. Greathouse and J. A. Killian, *Biochemistry*, 2002, **41**, 8396; (*c*) E. Pebay-Peyroula and J. P. Rosenbusch, *Curr. Opin. Struct. Biol.*, 2001, **11**, 427; (*d*) H. R. Ibrahim, U. Thomas and A. Pellegrini, *J. Biol. Chem.*, 2001, **276**, 43 767.

2 H. A. Rinia, J.-W. P. Boots, D. T. S. Rijkers, R. A. Kik, M. M. E. Snel, R. A. Demel, J. A. Killian, J. P. J. M. van der Eerden and B. de Kruijff, *Biochemistry*, 2002, **41**, 2814.

3 (*a*) J. A. Killian, *Biochim. Biophys. Acta*, 1998, **1376**, 401; (*b*) S. Morein, J. A. Killian and M. M. Sperotto, *Biophys. J.*, 2002, **82**, 1405.

4 L. K. Tamm, A. Arora and J. H. Kleinschmidt, *J. Biol. Chem.*, 2001, **276**, 32 399.

5 (*a*) H.-S. Won, S.-H. Park, H. E. Kim, B. Hyun, M. Kim, B. J. Lee and B.-J. Lee, *Eur. J. Biochem.*, 2002, **269**, 4367; (*b*) A. Rozek, C. L. Friedrich and R. E. W. Hancock, *Biochemistry*, 2000, **39**, 15 765

6 D. Stopar, R. B. Spruijt, C. J. A. M. Wolfs and M. A. Hemminga, *Biochim. Biophys. Acta*, 2003, **1611**, 5.

7 (*a*) J. A. Killian and G. von Heijne, *Trends Biochem. Sci.*, 2000, **25**, 429; (*b*) S. Persson, J. A. Killian and G. Lindblom, *Biophys. J.*, 1998, **75**, 1365; (*c*) S. H. White, W. C. Wimley, A. S. Ladokhin and K. Hristova, *Methods Enzymol.*, 1998, **295**, 62; (*d*) W. M. Yau, W. C. Wimley, K. Gawrisch and S. H. White, *Biochemistry*, 1998, **37**, 14 713.

8 (*a*) M. B. Ulmschneider and M. S. P. Sansom, *Biochim. Biophys. Acta*, 2001, **1512**, 1; (*b*) C. Landolt-Marticorena, K. A. Williams, C. M. Deber and R. A. F. Reithmeier, *J. Mol. Biol.*, 1993, **229**, 602.

9 R. Murari, M. M. A. Abd El-Rahman, Y. Wedmid, S. Parthasarathy and W. J. Baumann, *J. Org. Chem.*, 1982, **47**, 2158.

10 T. M. Dietz and T. H. Koch, *Photochem. Photobiol.*, 1987, **46**, 971.

11 L. J. Celewicz, *Photochem. Photobiol., B: Biology*, 1998, **43**, 66.

12 C. L. Norris, P. L. Meisenheimer and T. H. Koch, *J. Am. Chem. Soc.*, 1996, **118**, 5796.

13 J. Neel, *Pure App. Chem.*, 1972, **31**, 201.

14 K. A. Connors, *Binding Constants: The Measurement of Molecular Complex Stability*, John Wiley & Sons, 1987.

15 C. S. Wilcox, in *Frontiers in Supramolecular Organic Chemistry and Photochemistry*, eds. H.-J. Schneider and H. Dürr, VCH, Weinheim, 1991.

16 R. V. Pappu, R. K. Hart and J. W. Ponder, *J. Phys. Chem. B*, 1998, **102**, 9725, see also: http://dasher.wustl.edu/tinker/.

17 N. Foloppe and A. D. MacKerell, Jr., *J. Comput. Chem.*, 2000, **21**, 86.

18 J. J. P. Stewart, *J. Comput. Chem.*, 1989, **10**, 209.

19 G. Chessari, C. A. Hunter, C. M. R. Low, M. J. Packer, J. G. Vinter and C. Zonta, *Chem. Eur. J.*, 2002, **8**, 2860.

20 D. Wade, A. Boman, B. Wahlin, C. M. Drain, D. Andreu, H. G. Boman and R. B. Merrifield, *Proc. Natl. Acad. Sci. USA*, 1990, **87**, 4761.

21 (*a*) J. P. Gallivan and D. A. Dougherty, *J. Am. Chem. Soc.*, 2000, **122**, 870; (*b*) J. P. Gallivan and D. A. Dougherty, *Proc. Natl. Acad. Sci. USA*, 1999, **96**, 9459.

22 (*a*) G. K. Fukin, S. V. Linderman and J. K. Kochi, *J. Am. Chem. Soc.*, 2002, **124**, 8329; (*b*) J. Sunner, K. Nishizawa and P. Kebarle, *J. Phys. Chem.*, 1981, **85**, 1814.

23 D. L. Beene, G. S. Brandt, W. G. Zhong, N. M. Zacharias, H. A. Lester and D. A. Dougherty, *Biochemistry*, 2002, **41**, 10 262.

24 R. Olson, H. Nariya, K. Yokota, Y. Kamio and E. Gouaux, *Nat. Struct. Biol.*, 1999, **6**, 134.

25 Y. Satow, G. H. Cohen, E. A. Padlan and D. R. Davies, *J. Mol. Biol*, 1986, **190**, 593.